

Mesoscale ocean variability signal recovered from altimeter data in the SW Atlantic Ocean: a comparison of orbit error correction in three Geosat data sets

Gustavo GONI; Guillermo PODESTA; Otis BROWN & James BROWN

Division of Meteorology and Physical Oceanography, Rosenstiel School of Marine and Atmospheric Science,
University of Miami
(4600 Rickenbacker Causeway, Miami, Florida 33149-1098, USA)

● **Abstract:** Orbit error is one of the largest sources of uncertainty in studies of ocean dynamics using satellite altimeters. The sensitivity of GEOSAT mesoscale ocean variability estimates to altimeter orbit precision in the SW Atlantic is analyzed using three GEOSAT data sets derived from different orbit estimation methods: (a) the original GDR data set, which has the lowest orbit precision, (b) the GEM-T2 set, constructed from a much more precise orbital model, and (c) the Sirkes-Wunsch data set, derived from additional spectral analysis of the GEM-T2 data set. Differences among the data sets are investigated for two tracks in dynamically dissimilar regimes of the Southwestern Atlantic Ocean, by comparing: (a) distinctive features of the average power density spectra of the sea height residuals and (b) space-time diagrams of sea height residuals. The variability estimates produced by the three data sets are extremely similar in both regimes after removal of the time-dependent component of the orbit error using a quadratic fit. Our results indicate that altimeter orbit precision with appropriate processing plays only a minor role in studies of mesoscale ocean variability.

● **Resumo:** Erro orbital tem sido a principal fonte de incerteza no processamento de dados altimétricos. Recentes conjuntos de dados, baseados em modelos de predição orbital mais avançados e em novas metodologias de correção de erro, já foram capazes de reduzir o erro orbital de até uma ordem de magnitude em comparação com os GDRs originais. Neste trabalho nós avaliamos os resultados dessas melhores estimativas na descrição da variabilidade "meso-escalar" na parte sudoeste do oceano Atlântico Sul. Comparamos resultados obtidos em três conjuntos de dados: os GDRs originais e os conjuntos de dados GEM-T2 e Sirkes-Wunsch. Para garantir a "sensibilidade" das estimativas de variabilidade meso-escalar quanto às mudanças na precisão orbital, utilizamos as mesmas "correções ambientais" e o mesmo método de processamento de dados no tratamento dos três conjuntos de dados. Para investigar as possíveis diferenças entre os valores de variabilidade meso-escalar produzidos pelos três conjuntos de dados utilizamos as características espectrais dos residuais de "amplitude do mar" obtidas antes e depois da remoção do erro orbital "dependente" do tempo. O fato da componente meso-escalar do espectro quase não ter sido afetada pela remoção do maior comprimento de onda do sinal (o que corresponde principalmente ao erro orbital) sugere que muito pouco do sinal meso-escalar foi realmente removido através deste processo. Um "pico" menor no espectro da "faixa" B confirma uma variabilidade oceânica local menor com respeito à faixa A. Uma análise mais profunda demonstra que, após a remoção do erro orbital, os residuais de amplitude do mar são incrivelmente similares entre os três conjuntos de dados para uma determinada faixa. Tal resultado sugere que a precisão orbital contribui apenas parcialmente para o estudo da variabilidade meso-escalar oceânica. Esta conclusão só é válida se o erro orbital dependente do tempo puder ser removido sem se remover simultaneamente uma porção excessiva do sinal meso-escalar. Nossos resultados sugerem que estudos de variabilidade mesoescalar não requerem dados de órbita altimétrica extremamente precisos. Além disso, apesar deste trabalho só analisar dados do GEOSAT do oceano Atlântico Sul, acredita-se que tal resultado possa ser extrapolado para outras regiões do mar. Isto é devido às características espectrais do erro orbital dependente do tempo e à possibilidade de remoção deste erro sem remoção de grande parte do sinal meso-escalar oceânico. Estes resultados, contudo, não significam que não se deva tentar obter valores orbitais mais precisos. Pelo contrário, tal melhoramento pode ser capaz de levar à eliminação de algumas das limitações atualmente existentes na utilização de dados altimétricos. Por exemplo, estimativas de órbita do GEOSAT mais precisas nos permitiriam estudar a variabilidade oceânica em larga escala e, através de uma melhor compreensão do geóide, nos auxiliariam no estudo da circulação oceânica "meso e largo-escalar" geral.

● **Descriptors:** Altimetry, GEOSAT data sets, Orbit error, Mesoscale variability.

● **Descritores:** Altimetria, Conjunto de dados de GEOSAT, Erro orbital, Variabilidade mesoescalar.

Introduction

Satellite altimetry has been extensively applied to the study of ocean circulation. GEOSAT altimeter data have been used to investigate problems ranging from global circulation to fluctuations in western boundary currents (for example Chelton *et al.*, 1990; Nerem *et al.*, 1990; Vazquez *et al.*, 1990; Kelly & Gille, 1990; Qiu *et al.*, 1991). As part of a study of the Southwestern Atlantic which incorporates both *in situ* and satellite data, we explore the use of GEOSAT altimeter data to describe mesoscale oceanic variability in the region. Provost *et al.* (1989), Chelton *et al.* (1990), Stammer & Boning (1992), Forbes *et al.* (1993), and Provost & LeTraon (1993) used GEOSAT data to investigate variability of sea height and surface geostrophic currents in the South Atlantic Ocean.

Recent descriptions of the circulation and hydrography in the Southwestern Atlantic have been provided by Olson *et al.* (1988), and Peterson & Stramma (1991). The oceanic circulation in this region is dominated by the Brazil and Malvinas currents. The Brazil Current, the western boundary current associated with the subtropical gyre in the South Atlantic, flows south along the continental margin carrying warm subtropical waters until it separates from the coast at about 36° South. The cold subantarctic waters of the Malvinas Current flow north along the shelf break until they meet the Brazil Current in a region known as the Brazil-Malvinas Confluence. After its confluence with the Malvinas Current, the Brazil Current enters the South Atlantic interior in a series of large amplitude meanders. The Brazil-Malvinas Confluence region is associated with a complex mesoscale variability due to the displacement of frontal features.

The use of satellite altimetry involves the estimation of the height of the satellite with regards to a reference Earth ellipsoid. This height is determined through predictions from orbital models, which are periodically adjusted by tracking measurements from a limited number of ground stations. Despite the advances in orbit estimation procedures, errors in orbit determination are still a major source of uncertainty in GEOSAT sea height estimates. The spectral characteristics of the time-dependent orbit errors have recently been described by Chelton and Schlax (1993). It has been argued that a better orbit estimation method can produce more reliable estimates of the ocean dynamics (Haines *et al.*, 1990). To that effect, various GEOSAT data sets have been produced using different orbital estimation methods and corrections.

We will explore the sensitivity of mesoscale ocean variability estimates to altimeter orbit precision using three GEOSAT data sets based on different orbit estimation methods. We address this goal by analyzing the along-track spectral density of the sea height residuals and the

spatial-temporal patterns of sea height variability for two GEOSAT tracks in the Southwestern Atlantic Ocean.

Material and methods

GEOSAT data sets

We analyze the sea height variability along two descending GEOSAT tracks in the SW Atlantic, which extend from 15° to 60°S of latitude, and are approximately 5500 km long (Fig. 1). We choose two descending tracks since, in this area, descending tracks exhibit less data gaps than ascending tracks. The western track intersects the subtropical and subpolar western boundary flows, while the eastern track is chosen to sample a region with much weaker flows and less variability.

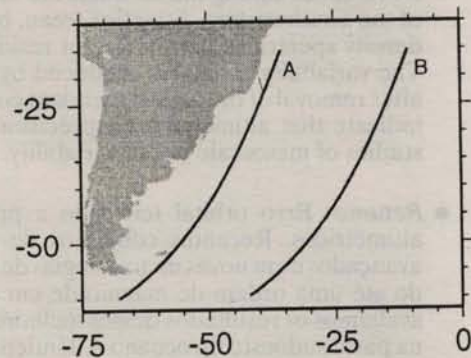


Fig. 1. Ground track locations for the two descending GEOSAT tracks analyzed in the South Atlantic Ocean.

The three GEOSAT data sets used in this study are the original Geophysical Data Records (GDRs), the GEM-T2 and the Sirkes-Wunsch data sets. The first two data sets were constructed using different orbit estimation methods, and the third data set was derived from spectral considerations of the GEM-T2 set. The radial ephemerides (orbit height) provided with the original GDRs were produced by the Naval Astronautics Group (NAG). The NAG orbits were derived using a relatively low-resolution gravity model, GEM-10, with an estimated rms radial accuracy of about 300 cm (Haines *et al.*, 1990). Recently, a new GEOSAT data set has been released which relies on orbit heights estimated by NASA's Goddard Space Flight Center using a more complete gravity model, GEM-T2. The GEM-T2 model yields estimates thought to be about an order of magnitude better than those of the NAG orbits. Sirkes and Wunsch (1990) generated an improved data set by computing additional orbit corrections based on the spectral characteristics of

the autocovariance function of corrected sea heights computed from the GEM-T2 data set.

At the time this research was done, only the first 40 cycles of the GEOSAT Exact Repeat Mission were available for the Sirkes-Wunsch data set. To ensure consistency in the comparisons, we analyze, for each of the three GEOSAT data sets, only these 40 cycles, encompassing the period November 1986 to September 1988.

Orbital errors

The GEOSAT orbital predictions in the three data sets described above still include two types of errors, time-dependent and time-invariant errors. The orbit error introduced by small changes in the orbit eccentricity is predominantly sinusoidal and time-dependent (Chelton *et al.*, 1990), with typical wavelengths of the order of one orbit (about 40,000 km). A usual approach for removing the time-dependent orbit error is to fit a given function (e.g., a sinusoid for long arcs, a polynomial for shorter arcs) to along-track sea surface height residuals. This method usually succeeds in eliminating most of the orbit error, although it may also remove part of the true oceanic variability mostly at longer spatial scales. Statistical considerations associated with the orbit error correction are explored by Le Traon *et al.* (1991). The second type of error, produced by irregularities in the gravitational field, is geographically constant at each track, and is referred to as time-invariant (Marsh & Williamson, 1980). Time-invariant errors are removed along with the geoid and the mean ocean circulation using the along-track collinear method.

GEOSAT data processing

Although improved environmental corrections are provided with the GEM-T2 data set, we want to investigate the effects of the various orbit ephemerides and orbit error correction methods. Therefore, we use the same set of environmental corrections for all three GEOSAT data sets. These corrections, provided in the original GDRs, are described in detail by Cheney *et al.* (1987) and include solid and ocean tides, wet and dry tropospheric, ionospheric, EM bias and inverse barometric corrections. The corrected heights are then interpolated onto a 7-km along-track grid. The interpolation results in ≈ 800 grid points, or bins, along each of the tracks.

A mean, or reference, sea surface profile for each track is computed using a slightly modified collinear approach, similar to that proposed by Chelton *et al.* (1990). This method produces a reliable estimate of the

mean sea level, by generating a curve constructed from the mean along-track slope of interpolated sea heights at fixed grid points, in a process equivalent to integration. Special attention is given to the treatment of data gaps, which are filled by interpolating the values at the edges of the gaps with a third order polynomial. We use the median and interquartile range values at each grid point as a data quality check, and exclude those values of along-track slope that lie beyond ± 4 interquartile ranges from the median. Sea height residuals are subsequently computed for each grid point and cycle by subtracting the reference estimate from the sea height values at each grid point. Note that the sum of the sea height residuals at each grid point is not zero, since they are referred to an integrated mean height profile, and not to the arithmetic mean profile. For this reason, it is more appropriate to refer to the integrated mean sea height profile as the reference profile. The subtraction of the reference profile automatically causes the elimination of the time-invariant orbit error.

The sea height residuals are still contaminated with the time-dependent orbit error, which must be estimated and removed from the signal. This error has a very long wave sinusoidal component that differs between tracks, and from cycle to cycle. A general approach to remove this orbit error is to fit a sinusoid or low order polynomial to the along-track sea height residuals for each cycle. This method assumes that the error is purely periodic and deterministic. For long tracks ($> 10,000$ km), a sinusoid is usually considered the best choice. For shorter tracks, a linear or quadratic polynomial is generally accepted as a good alternative for removing the time-dependent orbit error. The choice of the order of the polynomial is related to the length of the track. First-order polynomials are usually recommended for tracks shorter than 3000 km (Chelton *et al.*, 1990, and Le Traon *et al.*, 1991). Given the length of the arcs (5500 km), we use a quadratic weighted fit to remove the time-dependent orbit error in all the data sets. To minimize the chance of grid points with higher temporal variability having a greater influence in the polynomial fit, the adjustment is done by weighting the fit by the inverse of the variance (Kelly *et al.*, 1991). Polynomial adjustments usually do not perform well at the ends of the tracks, introducing some additional variability to the sea height residuals at these locations. This situation does not significantly affect our spectral analyses because the first and last 10% of the tracks are tapered with a cosine window. In the subsequent analyses, we compute and compare the sea height residuals with and without removing the time-dependent orbit error. We then use spectral methods to estimate the magnitude of the mesoscale and large scale signals removed from the residuals by the polynomial adjustment procedure.

Results and discussion

Sea height residuals

The sea height residuals, after the polynomial orbit correction, reveal that the tracks analyzed transect areas of different oceanographic characteristics. Figures 2a and 3a show the sea height residuals for tracks A and B, for the first 40 cycles of the GDR data set. Note that for this analysis the sea height residuals are filtered using a low-pass filter with a cut-off frequency of 40 km, which approximately corresponds to the GEOSAT instrument noise (Flament *et al.*, 1989). The rms sea height variability for track A (Fig. 2b) varies from 6 cm at low latitudes (15 to 25°S) to more than 30 cm at about 42°S. The area of maximum variability is found where the track crosses the extension of the Brazil-Malvinas confluence. The maximum amplitude of sea height residuals in this region can reach about 70 cm. A second area of high variability, although less pronounced, is found between 55 and 58°S and corresponds to the edge of the Antarctic Circumpolar Current (ACC). Track B transects a region of much lower variability, where the influence of the Brazil Current extension is less pronounced. The highest rms variability values of around 20 cm are observed at 50°S (Fig. 3b) and correspond to the edge of the ACC.

Our estimates of rms sea height variability are slightly higher than those obtained by Forbes *et al.* (1993), as a consequence of not having damped the sea height variability results by interpolating them onto a much larger grid. Our estimates of horizontal sea height variations are comparable to the *in situ* estimates in the Argentine basin reported by Roden (1986), obtained by dividing the dynamic height differences by the gravity acceleration. The *in situ* height differences are found to be of the order of 20 to 40 cm over distances of 100 km.

Orbit error corrections for each bin along-track can be visualized by calculating the difference between the sea height residuals before and after the orbit correction is made. These estimates for tracks A and B are shown for all data sets in Figure 4. The orbit error corrections are highest for the original GDR data set, which is indicative of its lowest orbit precision. The amplitude of the orbit correction values is lower for the GEM-T2, and even lower for the Sirkes-Wunsch data set, reflecting the progressive improvement in orbit estimation with respect to the GDR data set. The space-time average amplitude of the time-dependent orbit corrections are ≈ 50 cm (track A) and ≈ 60 cm (track B) for the GDR, ≈ 13 cm (A) ≈ 15 cm (B) for the GEM-T2, and, ≈ 9 cm (A) and ≈ 8 cm (B) for the Sirkes-Wunsch data set.

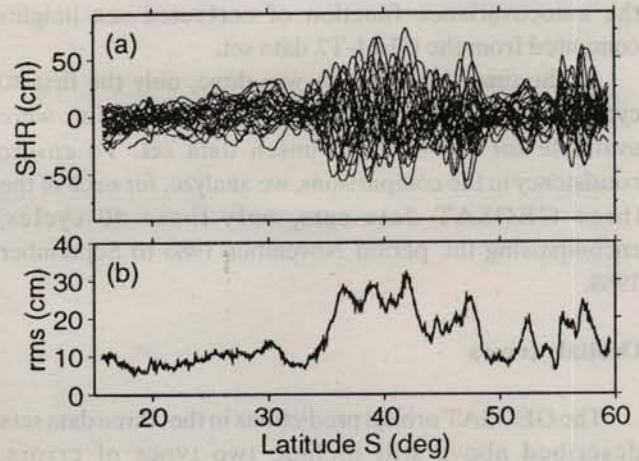


Fig. 2. (a) Low-passed sea height residual (SHR) profiles for track A generated from the first 40 GEOSAT cycles, using the GDR data set. The residuals are computed by first removing the reference sea height profile from each individual corrected profile. The time-dependent orbit error is then removed by subtracting a weighted second-order polynomial from the residuals, which are finally filtered using a bell-shaped cosine window. (b) rms sea height variability for the above residuals.

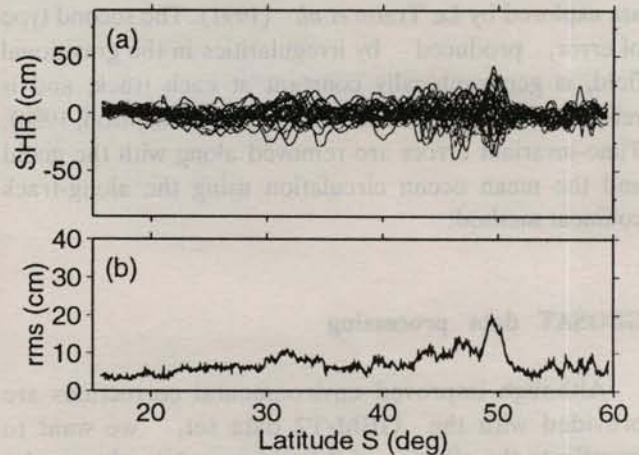


Fig. 3. Same as Figure 2, for track B.

Along-track wavenumber spectra

The polynomial orbit correction method can remove true long-scale oceanic signal along with the time-dependent orbit error. More important for our objectives is the possibility of excessive removal of mesoscale oceanic signal, or "overfitting", along with the orbit error. To assess how much mesoscale oceanic signal is removed by the orbit correction procedure, we analyze the spectral characteristics of the sea height residuals before and after the polynomial adjustment.

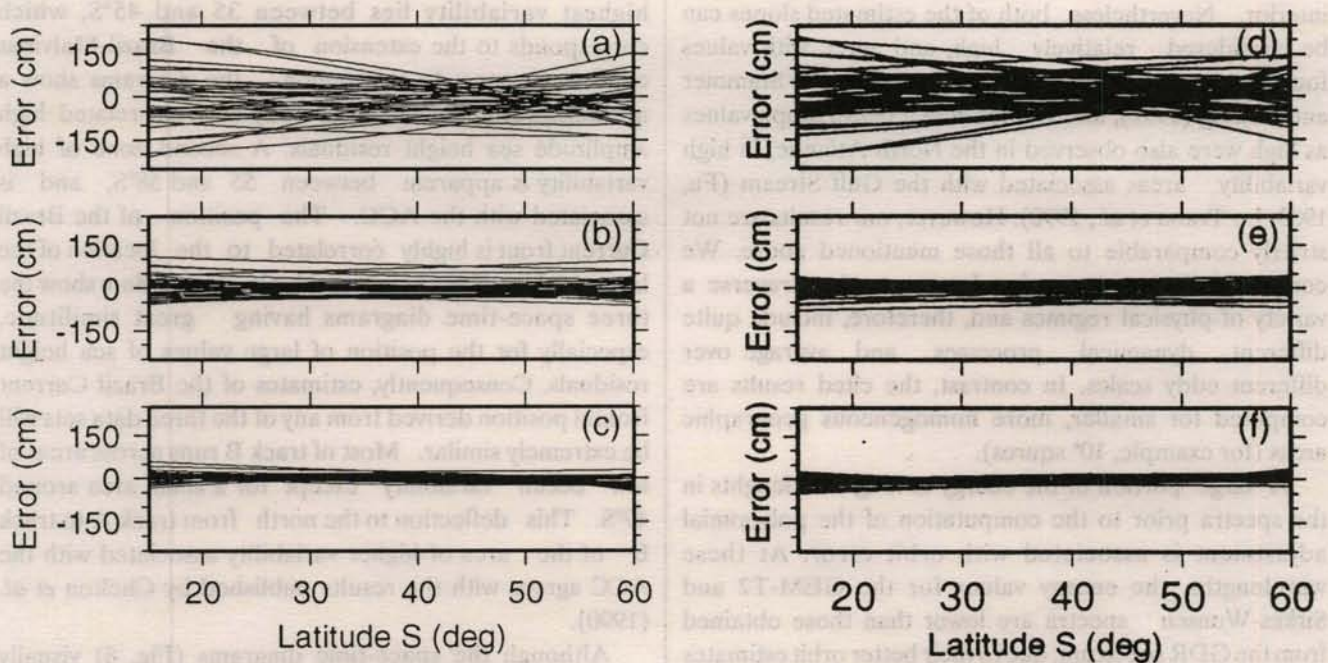


Fig. 4. Estimated magnitude of the long wavelength time-dependent orbit corrections for tracks A and B, (a and d) GDR set, (b and e) GEM-T2 set, and (c and f) Sirkes-Wunsch set. The space-time average amplitude of the corrections are about 50 cm and 60 cm for the GDR, 13 cm and 15 cm for the GEM-T2 and 9 cm and 8 cm for the Sirkes-Wunsch data sets, for tracks A and B.

The along-track mean wavenumber power density spectra of the sea height residuals is computed for each of the data sets. In order to avoid excessive damping in the signal at mesoscale wavelengths, the sea height residuals are not low-pass filtered for this analysis. The Fast Fourier technique, commonly used to compute wavenumber spectra, requires the data to be evenly spaced and without missing values. Due to the existence of data gaps in all the cycles, we compute the spectra using the Lomb-Scargle method (Press & Teukolsky, 1988) which handles this situation very efficiently. Only one cycle in track A (day 194 of 1988) has very few observations and is not used in the spectral analysis.

The power density spectrum is first computed separately for each track and cycle. To avoid leakage into higher frequencies, 10% of the signal at each end of every cycle is tapered by multiplying the sea height residuals by a cosine-bell window. A mean power density spectrum is then computed for each track by averaging the individual spectra. The highest frequency which can be detected from data spaced at intervals θ_0 apart is the Nyquist frequency, $N_q = (2\theta_0)^{-1}$, i.e., $N_q = 0.07 \text{ km}^{-1}$.

Figures 5 and 6 show the spectra for each of the data sets, before and after removing the time-dependent orbit error for the two tracks analyzed. The spectra prior to the long-wavelength orbit error removal are mostly red, with most of the energy concentrated at wavelengths larger

than 1000 km, which reflects the influence of the time-dependent orbital error. For wavelengths between 60 and 1000 km, mesoscale oceanic variability dominates the spectra. At wavelengths shorter than 60 km the spectra change from red to white, and the band-limited instrument noise dominates the spectra. The detection limit of ocean variability at short-wavelengths is given by the location of this white noise frequency band. The sea height residuals that correspond to this uncorrelated signal, or white noise, have an rms variability of about 5 cm.

The spectra of the sea height residuals can be characterized by two parameters: the peak at which the spectral density begins its main decrease, and the slope of the red part of the spectrum. After the polynomial adjustment, the power density value of the peaks is higher in track A than in track B (Figs 5b and 6b), with values of approximately 2×10^4 and $1 \times 10^4 \text{ cm}^2 / \text{cpkm}$, respectively. This clearly reflects the existence of higher variability in the area of the extension of the Malvinas and Brazil currents. The spectra slope value are proportional to k^{-5} and k^{-4} , for track A and B, respectively. The lower slope value for track B, indicative of a less energetic spectrum, confirms the lower oceanic variability in this area. An analysis of all tracks located between tracks A and B reveals that the decrease in the slope is progressive, suggesting a drop in eddy height variability as one moves from the energetic western boundary to the basin

interior. Nevertheless, both of the estimated slopes can be considered relatively high, and agree with values found in recent studies of the same area by Stammer and Boning (1992), and Forbes *et al.* (1993). Slope values as high were also observed in the North Atlantic, in high variability areas associated with the Gulf Stream (Fu, 1983; Le Traon *et al.*, 1990). However, our results are not strictly comparable to all those mentioned above. We computed the spectra using long arcs that traverse a variety of physical regimes and, therefore, include quite different dynamical processes and average over different eddy scales. In contrast, the cited results are computed for smaller, more homogeneous geographic areas (for example, 10° squares).

A large portion of the energy at long wavelengths in the spectra prior to the computation of the polynomial adjustment is associated with orbit error. At these wavelengths, the energy values for the GEM-T2 and Sirkes-Wunsch spectra are lower than those obtained from the GDR spectrum, due to their better orbit estimates (Figs 5a and 6a). However, for mesoscale wavelengths between 60 and 1000 km, the spectra for the three data sets are very similar. For wavelengths lower than 60 km, noise is dominant in all of the spectra. After removing the orbit error, most of the energy at wavelengths larger than 1000 km disappears (Figs. 5b and 6b). For wavelengths between 60 and 1000 km, the spectra remain almost unchanged, suggesting that not much mesoscale signal was removed by the polynomial adjustment.

Figure 7 shows the along-track power density spectra of the estimated time-dependent orbit error, i.e., the second order polynomial removed at each track for the three data sets. These spectra confirm that the energy removed at mesoscale wavelengths is almost negligible. Therefore, we feel confident that the polynomial adjustment used in this study does not affect significantly our estimates of mesoscale variability, allowing meaningful oceanographic interpretations.

Space time variability

After having removed the time-dependent orbit error, our main interest now lies in comparing the remaining oceanographic mesoscale signal at each track for three data sets. This is done by analyzing the low-pass filtered sea height residuals. Figures 8a, 8b and 8c show space-time diagrams of sea height residuals along track A for three data sets after the time-dependent orbit error correction. Figures 8d, 8e and 8f show the corresponding diagrams for track B. The black areas in the figures correspond to bins with no data, or values eliminated during the data quality check. For track A, the area of

highest variability lies between 35 and 45°S , which corresponds to the extension of the Brazil-Malvinas confluence zone. In this region, the diagrams show a northeastward movement of eddy-or front-related high amplitude sea height residuals. A second zone of high variability is apparent between 55 and 58°S , and is associated with the ACC. The position of the Brazil Current front is highly correlated to the location of the largest values of sea height residuals. Figures 8a-c show the three space-time diagrams having great similitude, especially for the position of large values of sea height residuals. Consequently, estimates of the Brazil Current frontal position derived from any of the three data sets will be extremely similar. Most of track B runs across areas of low ocean variability except for a small area around 49°S . This deflection to the north from track A to track B of the area of higher variability associated with the ACC agrees with the results published by Chelton *et al.* (1990).

Although the space-time diagrams (Fig. 8) visually show a striking similarity for the three data sets, differences can be quantified. We compute, bin by bin, the differences between sea height residuals for the two improved data sets (GEM-T2 and Sirkes-Wunsch) and the GDRs. Histograms of the differences for all the cycles are shown in Figure 9. The number of bins compared is about 26,000 for each track. In all cases, the distribution of differences between the data sets is centered around 0 cm, indicating the absence of any systematic differences among the sets. The histograms of the GEM-T2 minus GDRs differences of sea height residuals show a larger spread than the corresponding figures for the Sirkes-Wunsch minus GDRs differences. Further examination reveals that the highest absolute differences correspond, in most cases, to the extremes of the tracks, where polynomial adjustments are known to be more variable.

One unexpected result of this study is the considerable residual orbit error in the Sirkes-Wunsch data set. The orbit errors in this set were supposed to have been minimized. They have been used in at least one study of the Gulf Stream (Ezer *et al.*, 1993) without additional adjustments. Although the error is smaller than in the GDR and GEM-T2 sets, we found that the Sirkes-Wunsch data had to be corrected through the polynomial adjustment before they could be used for studies of mesoscale ocean variability. Once the corrections are applied, the variability estimates from all three data sets are very similar, with differences among sets being small in relation to the overall error of the measurements. This result is not unexpected (Chelton and Schlax, 1993; Tai, 1989) given the long wavelength of the time-dependent orbit error, although we have not seen this result quantified to date.

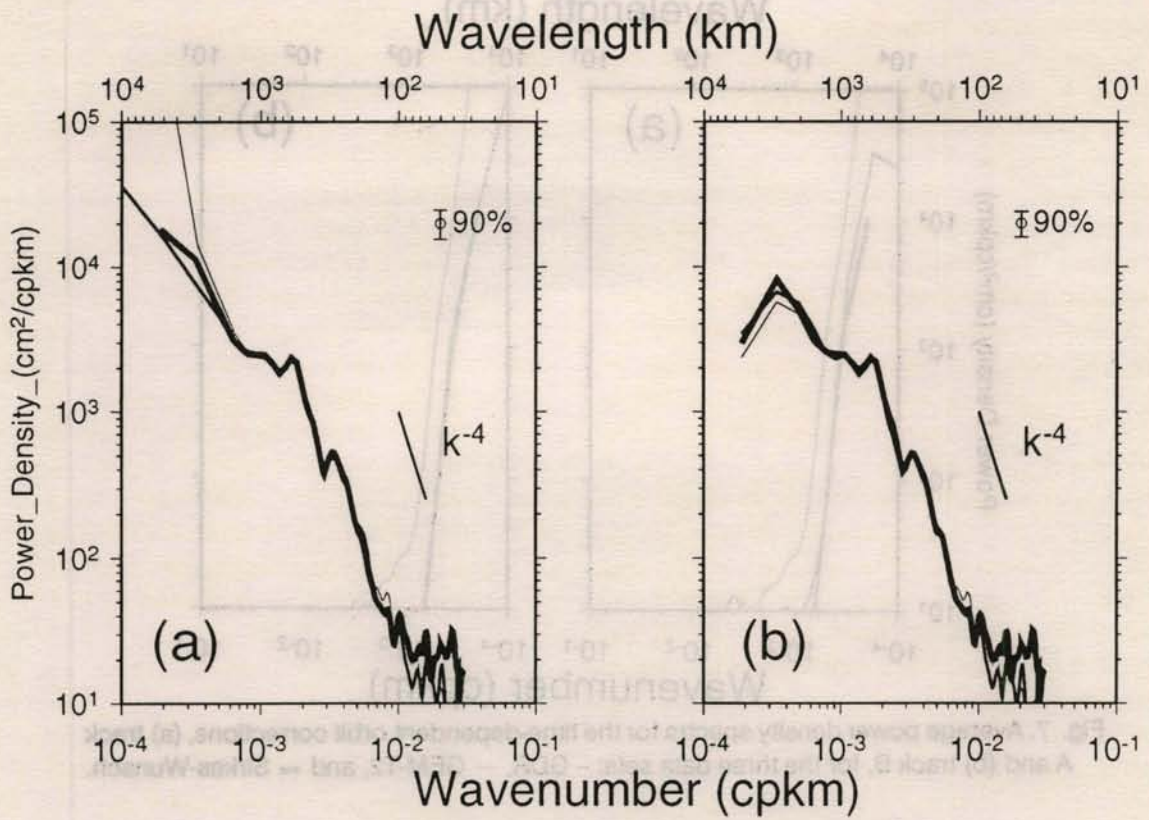


Fig. 5. Average power density spectra of the sea height residuals for track A, for the three data sets (- GDR, — GEM-T2, and - Sirkes-Wunsch): (a) Before the orbit error correction and (b) after the orbit error correction. The error bar represents 95% confidence limits, and the solid line typifies the mean slope for mesoscale wavelengths.

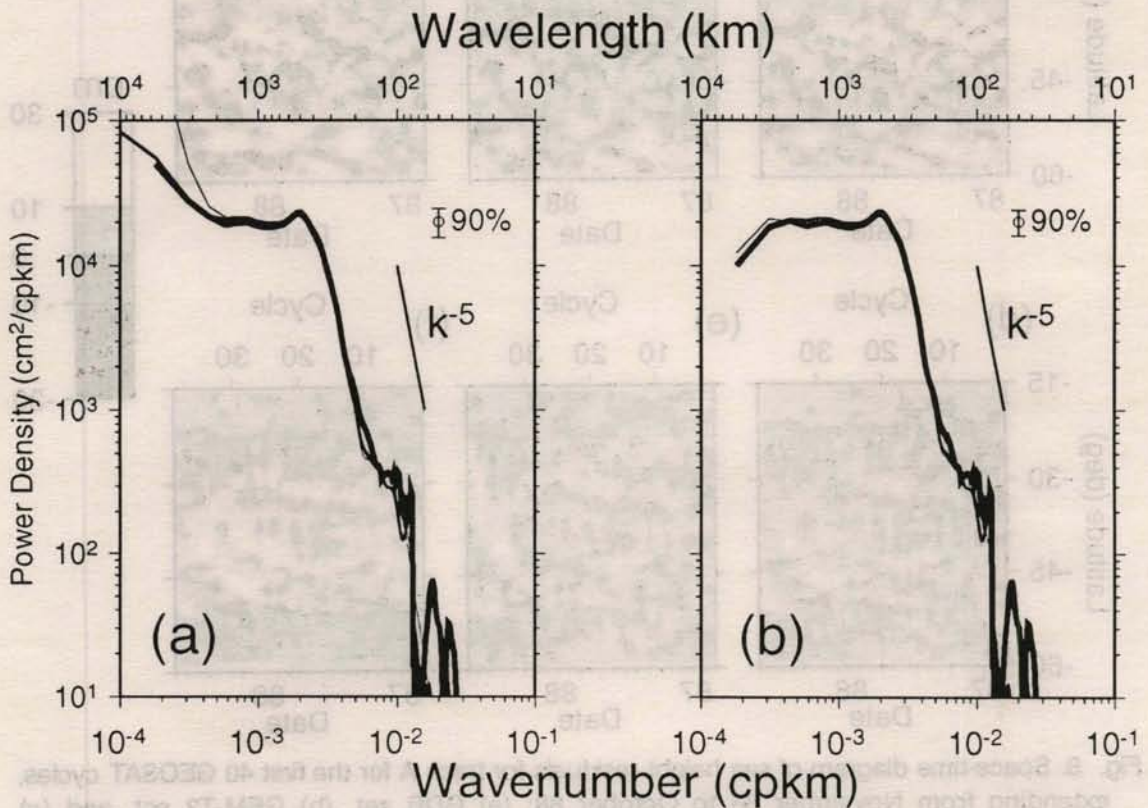


Fig. 6. Same as Figure 6 for track B.

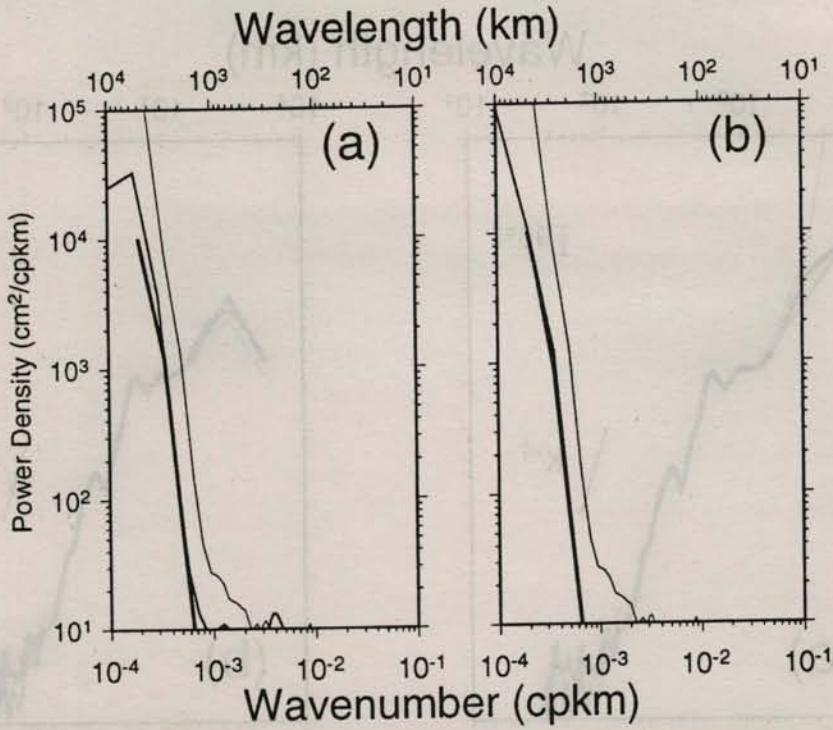


Fig. 7. Average power density spectra for the time-dependent orbit corrections, (a) track A and (b) track B, for the three data sets: - GDR, - GEM-T2, and - Sirkes-Wunsch.

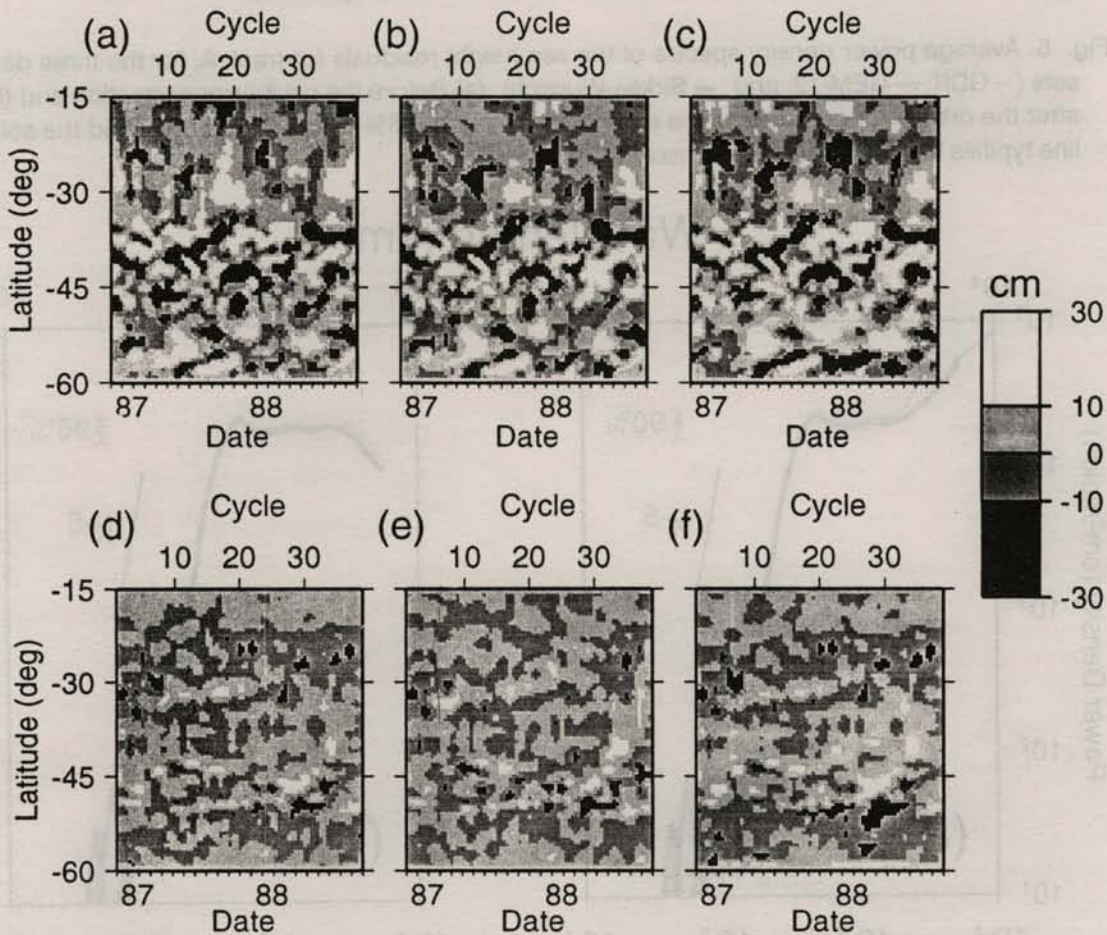


Fig. 8. Space-time diagram of sea height residuals for track A for the first 40 GEOSAT cycles, extending from November 86 to October 88: (a) GDR set, (b) GEM-T2 set, and (c) Sirkes-Wunsch set; and track B: (d) GDR set, (e) GEM-T2 set, and (f) Sirkes-Wunsch set.

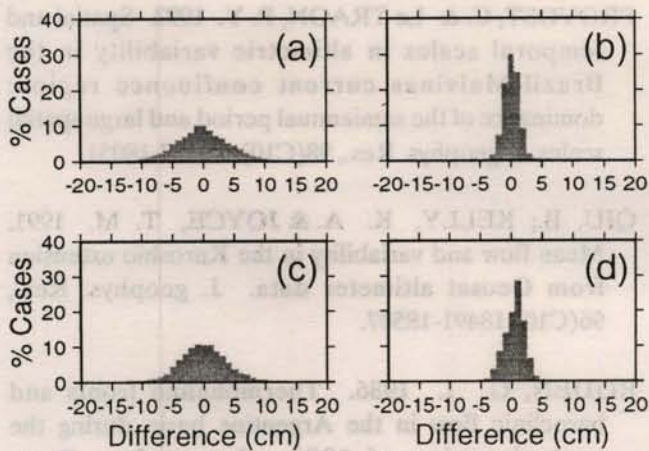


Fig. 9. Histograms of bin-by-bin differences in sea height residuals between the data sets: (a) GEM-T2 minus GDR, track A, (b) Sirkes-Wunsch minus GDR, track A, (c) GEM-T2 minus GDR, track B, and (d) Sirkes-Wunsch minus GDR, track B.

Conclusions

Improvements in altimeter orbit error estimation to the original GEOSAT data set lead to the construction of two new data sets, the GEM-T2 and Sirkes-Wunsch data sets. The sensitivity of mesoscale variability estimates using these three different GEOSAT data sets is investigated by comparing characteristics in their sea height residuals power density spectra and space-time diagrams. After removing the long wavelength component of the spectra remains almost unchanged. Further analysis shows that the mesoscale signal recovered from each data set is approximately the same. However, improvements in the orbit estimation are still necessary in order to study large scale ocean variability.

Acknowledgements

This work was partially supported by NASA grant NAGW-273 (GJG, OBB) NFS grant OCE9102112 (GPP), NASA grant NAS5-31361, ONR grant N0001489J1144 (OBB, GJG, JWB), and NASA grant NAS5-31362(JWB).

We would like to thank Dr Ziv Sirkes (INO) and Dr Don Collins (NOAA/NODC) for providing the data sets used in this study. We greatly appreciate the help provided by Mr. Angel Li and Ms. Joanie Splain during the early processing of the GEOSAT data, by Dr Donald Olson for his comments on the manuscript, and by Aline Kroger for the help in translating the abstract into Portuguese. The comments provided by Dr Harry de Ferrari for the spectral

calculations are greatly appreciated. We also appreciate the suggestions by the anonymous reviewers. The GMT-System software, developed by P. Wessel (University of Hawaii) and W. Smith (University of California at San Diego), was used to generate all plots.

References

- CHELTON, D. B.; SCHLAX, M. G., WITER, D. L. & RICHMAN, J. G. 1990. Geosat altimeter observations of the surface circulation of the southern ocean. *J. geophys. Res.*, 95(C10): 17877-17903.
- _____ & SCHLAX, M. G. 1993. Spectral characteristics of time-dependent orbit errors in altimeter height measurements. *J. geophys. Res.*, 98 (C7):12579-12600.
- CHENEY, R. E.; DOUGLAS, B. C.; AGREEN, R. W.; MILLER, L.; PORTER, D. L. & DOYLE, S. N. 1987. Geosat altimeter geophysical data record: user handbook. NOAA Technical Memorandum NOS NGS-46.
- EZER, T.; MELLOR, G. L.; KO, D-S. & SIRKES, Z. 1993. Comparison of gulf stream sea surface height fields derived from Geosat altimeter data and those derived from sea surface temperature data. *J. atmos. ocean. Technol.*, 10(1):76-87.
- FLAMENT, P.; KORSO, P.M. & HUYER, A. 1989. Mesoscale variability off California as seen by the GEOSAT altimeter. *Proc. IGARSS'89, I.E.E.E.* p. 1063-1068.
- FORBES, M. C.; LEAMAN, K.; OLSON, D. & BROWN, O. 1993. Eddy and wave dynamics in the South Atlantic as diagnosed from GEOSAT altimeter data. *J. geophys. Res.*, 98(C7): 12297-12314.
- FU, L-L. 1983. On the wave number spectrum of oceanic mesoscale variability observed by the SEASAT altimeter. *J. geophys. Res.*, 88(C7):4331-4341.
- HAINES, B. J.; BORN, G. H.; ROSBOROUGH, G. W.; MARSH, J. G. & WILLIAMSON, R. G. 1990. Precise orbit computation for the Geosat exact repeat mission. *J. geophys. Res.*, 95(C3): 2871-2885.
- KELLY, K. A. & GILLE, S. T. 1990. Gulf stream surface transport and statistics at 69°W from the Geosat altimeter. *J. geophys. Res.*, 95(C3):3149-3161.

- KELLY, K. A.; JOYCE, T. M.; SCHUBERT, D. M. & CARUSO, M. J. 1991. The mean sea surface height and geoid along the Geosat subtrack from Bermuda to Cape Cod. *J. geophys. Res.*, 96(C7): 12699-12709.
- Le TRAON, P. Y.; ROUQUET, M. C. & BOISSIER, C. 1990. Spatial scales of mesoscale variability in the North Atlantic as deduced from Geosat Data. *J. geophys. Res.*, 95(C11): 20267-20285.
- _____; BOISSIER, C. & GASPAR, P. 1991. Analysis of errors due to polynomial adjustment of altimeter profiles. *J. atmos. ocean. Technol.*, 8(3): 385-396.
- MARSH, J. G. & WILLIAMSON, R. G. 1980. Precision orbit analyses in support of the Seasat altimeter experiment. *J. astronaut. Sci.*, 28:345-369.
- NEREM, R. S.; TAPLEY, B. D. & SHUM, C. K. 1990. Determination of the ocean circulation using Geosat altimetry. *J. geophys. Res.*, 95(C3): 3163-3179.
- OLSON, D. B.; PODESTÁ, G. P.; EVANS, R. H. & BROWN, O. B. 1988. Temporal variations in the separation of Brazil and Malvinas currents. *Deep-sea Res.*, 35:1971-1990.
- PETERSON, R. G. & STRAMMA, L. 1991. Upper-level circulation in the South Atlantic ocean. *Prog. Oceanogr.*, 26(1):1-73.
- PRESS, W. H. & TEUKOLSKY, S. A. 1988. Search algorithm for weak periodic signals in unevenly spaced data. *Computers, Physics*, Nov and Dec, p. 77-82.
- PROVOST, C.; GARÇON, V. & GARZOLI, S. 1989. Sea level variability in the Brazil and Malvinas confluence region. *Adv. Space Res.*, 9:7387-7392.
- PROVOST, C. & Le TRAON, P. Y. 1993. Spatial and temporal scales in altimetric variability in the Brazil-Malvinas current confluence region: dominance of the semiannual period and large spatial scales. *J. geophys. Res.*, 98(C10): 18037-18051.
- QIU, B.; KELLY, K. A. & JOYCE, T. M. 1991. Mean flow and variability in the Kuroshio extension from Geosat altimeter data. *J. geophys. Res.*, 96(C10):18491-18507.
- RODEN, G. I. 1986. Thermohaline fronts and baroclinic flow in the Argentine basin during the austral spring of 1984. *J. geophys. Res.*, 91(C4):5075-5093.
- SIRKES, Z. & WUNSCH, C. 1990. Note on apparent systematic and periodic errors in Geosat orbits. *Geophys. Res. Letts*, 17:1307- 1310.
- STAMMER, D. & BONING, C. W. 1992. Mesoscale variability in the Atlantic ocean from Geosat altimetry and WOCE high-resolution numerical modelling. *J. phys. Oceanogr.*, 22(7): 732-752.
- TAI, C. K. 1989. Accuracy assessment of widely used orbit error approximations in satellite altimetry. *J. atmos. ocean. Technol.*, 6(1):147-150.
- VAZQUEZ, J.; ZLOTNICKI, V. & FU, L-L. 1990. Sea level variabilites in the gulf stream between Cape Hatteras and 50°W: a Geosat study. *J. geophys. Res.*, 95(C10): 17957-17964.